N69-17792

PART I: SUMMARY REPORT: FURTHER STUDIES OF THE COUPLED CHEMICALLY REACTING BOUNDARY LAYER AND CHARRING ABLATOR - PART II: AN EVALUATION OF SURFACE RECESSION MODELS FOR THE APOLLO HEAT SHIELD MATERIAL - PART III: A NONGREY RADIATION TRANSPORT MODEL SUITABLE FOR USE IN ABLATION-PRODUCT CONTAMINATED BOUNDARY LAYERS - PART IV: NONSIMILIAR SOLUTION OF AN INCOMPRESSIBLE TURBULENT BOUNDARY LAYER BY AN INTEGRAL MATIRIX METHOD

E. P. Bartlett, et al

ABSTRACT

A numerically-accurate solution technique is introduced for the prediction of constant property turbulent boundary layer characteristics. The procedure can be termed a strip integral technique in that approximating functions (splined cubics) are used to represent the primary variables across boundary layer strips, and the governing equations are integrated across the strips. That is, squarewave weighting functions are used in forming the integrals of the governing equations. Derivatives in the normal direction are related to one another by Taylor series truncated to reflect the cubic approximation. Implicit quadratic finite difference relations are used to express streamwise derivatives for nonsimilar solutions. The turbulent model employs the idea of a wall and a wake region. In the wall region, a mixing length model for eddy viscosity is used, the mixing length being described by a first-order differential equation. The effects of wall injection or suction are considered in the mixing length equation. The wake region model employs a constant eddy viscosity at each streamwise station. Eddy viscosity in this region is taken to be proportional to the free stream velocity and the displacement thickness.

The resultant set of linear and nonlinear algebraic relations is solved by general Newton-Raphson iteration using an efficient matrix inversion technique. Portions of the matrix contain coefficients involving grid spacing only; therefore, these need be inverted only once for a given problem. Use of the splined cubic interpolation functions allows accurate solutions with relatively few (around twelve) nodes through the boundary layer. Typically, three or four iterations are required to reach a converged solution for a typical streamwise step.

FOREWORD

The present report is one of a series of four reports, published simultaneously, which describe extension and application of analyses and computational procedures for predicting the in-depth response of charring ablation materials and nonsimilar chemically reacting boundary layers which were generated under a previous contract (NAS9-4599). In particular, the present reports describe the extension of a laminar multicomponent chemically-reacting (equilibrium) boundary-layer program to include nongrey radiation coupling, the extension of this computational procedure to turbulent flow (at this point for incompressible flows only), the further checkout of a code which couples the laminar boundary layer procedure to a transient charring ablation code, and the application of these and other computational procedures to the Apollo heat shield material and typical Apollo missions. Part I serves as a summary report and describes the present status of and solutions obtained with the various computational procedures. In Part II a thermochemical ablation program based on a transfer-coefficient approach is utilized to investigate ablation mechanisms for the Apollo heat shield material. The radiation transport model which is utilized is described in Part III, whereas the turbulent boundary layer code is discussed in Part IV.

The titles in the series are:

Part I: Summary Report: Further Studies of the Coupled Chemically Reacting Boundary Layer and Charring Ablator, by E.P. Bartlett, W.E. Nicolet, L.W. Anderson, and R.M. Kendall.

Part II: An Evaluation of Surface Recession Models for the Apollo Heat Shield Material, by E.P. Bartlett, and L. W. Anderson.

Part III: A Nongrey Radiation Transport Model Suitable for Use in Ablation-Product Contaminated Boundary Layers, by W. E Nicolet

Part IV: Nonsimilar Solution of an Incompressible Turbulent Boundary Layer by an Integral Matrix Method, by L. W. Anderson and R. M. Kendall.

This effort was conducted for the Structures and Mechanics Division of the Manned Spacecraft Center, National Aeronautics and Space Administration under Contract NAS9-6719 with Mr. Donald M. Curry as the NASA Technical Monitor. Development of the turbulent boundary layer code was sponsored jointly by NASA/MSC and by the Air Force Weapons Laboratory, Kirtland Air Force Base, with Lt. Ronald H. Aungier as Project Engineer. Extension of the turbulent boundary layer analysis to compressible flows is continuing under AFWL sponsorship. Mr. Eugene P. Bartlett of Aerotherm Corporation was Program Manager and Principal Investigator for the efforts reported here.

TABLE OF CONTENTS

LIST OF FIGURES

LIST OF SYMBOLS

C	constant introduced in the α constraint (Equation 25)
C_f	coefficient of drag, $2\tau_o/\rho_1 u_1^2$
d_o, d_1, d_2	coefficients defined in finite-difference representation of streamwise derivatives (Equations (47) and (48) for two and three point difference relations, respectively)
f	stream function (defined by Equation (22))
H	boundary layer shape parameter, δ^*/θ
K	constant in Prandtl mixing length expression
ℓ	mixing length
N	number of nodal points
p	pressure
r_o	local radius of body in a meridian plane for an axisymmetric shape
Re	Reynolds number, $u_1 s/\nu$
s	distance along body from stagnation point or leading edge
u	velocity component parallel to body surface
u_τ	shear velocity, $\sqrt{\tau_o/\rho}$
v	velocity component normal to body surface
y	distance from surface into boundary layer, measured normal to the surface
y^+	normalized y defined as yu_τ/ν
$\bar{y}$	normalized y defined as y/δ
y_a^+	constant in mixing length equation
α	normalizing parameter used in definition of η defined implicitly by the use of a constraint such as Equation (26).
β	streamwise pressure gradient parameter, $2\frac{d \ln u_1}{d \ln \xi}$
$\ell_{\ell}-\ell_{\ell-1}$	logarithmic distance between two streamwise positions denoted by the subscripts ℓ and $\ell-1$

LIST OF SYMBOLS (Continued)

δ	boundary layer thickness
δ^*	boundary layer displacement thickness
ε	eddy viscosity
ε_1	eddy viscosity found from wall region expression
ε_2	eddy viscosity found from wake region expression
η	transformed coordinate in a direction normal to the surface, defined by Equation (23)
θ	momentum thickness
μ	shear viscosity
ν	kinematic viscosity
ξ	transformed streamwise coordinate, defined by Equation (28)
ρ	density
τ	shear stress
ϕ	turbulent intermittency

SUBSCRIPTS

i	i^{th} node
ℓ	ℓ^{th} station
o	wall
1	boundary layer edge
θ	based on momentum thickness

SUPERSCRIPTS

κ	equal to unity for axisymmetric bodies and zero for two-dimensional bodies
$'$	represents partial differentiation with respect to η. Also indicates a fluctuating quantity in turbulence expressions

SECTION 1

INTRODUCTION

A computational procedure is described herein which is suitable for obtaining accurate numerical solutions of the constant property, nonsimilar, single-component turbulent boundary layer equations with arbitrary fluid injection at the boundary. A Fortran IV computer program, designated the SAINT program for Strip Analysis of Incompressible Nonsimilar Turbulent boundary layers, has been developed in accordance with this analysis and is described in Appendix A.

The turbulent boundary layer procedure described here represents a simplification and an extension of the laminar boundary layer procedure presented by Kendall and Bartlett (Reference 1). The simplification involves the environmental generality embodied in the laminar procedure (general chemistry, unequal diffusion and thermal diffusion of all species, coupled wall boundary condition, etc.). The extension includes the modification of the coordinate transformation to treat the turbulent boundary layer more appropriately, and the introduction of a turbulent model. The analysis and computer program described here are currently being extended to include the general chemistry and other features of Reference 1.* In view of the intended final result, a minimization of the number of boundary-layer nodal points required to obtain a solution was judged to be of prime importance as a consequence of the relatively large times associated with state calculations for a general chemical environment and, in the streamwise direction, because of the desire to couple the boundary layer procedure to a transient internal conduction or ablation solution.

*This is being performed under the sponsorship of the Air Force Weapons Laboratory (see Foreword).

For a given accuracy, the number of necessary "nodal points" in the surface normal direction is controlled primarily by the nature of the functions which relate the dependent variables (and their derivatives) to the independent variable. Thus the smooth functions typically used in integral relations approaches require fewer "nodal points"* than the functions with discontinuous first derivatives implied by most finite difference approximations. In order to permit relatively flexible profiles, connected cubics were selected to represent streamwise velocity. The first and second derivatives of these cubics were made continuous at the connecting points. The advantages of such a "spline fit" are considered, for example, in Reference 4.

Following the general integral relations approach, weighting functions must be selected. In the present study, as in Reference 1, step weighting functions similar to those used by Pallone (Reference 2) were adopted. That is to say, the momentum equation is integrated between nodal points (over strips), with a unity weighting function.

In the past when relatively large spacing in the streamwise direction has been desired, iterative procedures have generally been used to assure accuracy and stability. Some of these procedures have treated the solution in a manner resembling those used for similar solutions but with the addition of finite difference representations for the nonsimilar terms, a procedure which eliminates the necessity of special starting techniques. Using this basic approach, the specific treatment adopted in the current study follows most closely the matrix procedure used by Leigh (Reference 5), wherein the iteration is a consequence of the solution of a set of linear and nonlinear algebraic relations. Whereas a special successive approximation procedure was used by Leigh, however, the general Newton-Raphson technique is used in the present procedure. This technique results in linearized coupling between all relations required to characterize the boundary layer, and thus assures a more general, rapid, and stable iterative convergence.

*The term "nodal point" is meant to encompass the integral strips of Pallone (Reference 2) and the matching points used by Dorodnitsyn (Reference 3).

The basic equations for a turbulent boundary layer are described in Section 2. These are treated in a manner similar to the method used by Clauser (Reference 6), in which the flow is divided into wall and wake regions. In the wall region, a mixing length model is introduced which accounts for the variable shear due to injection. In the wake region, the eddy viscosity is taken to be constant at a given streamwise station and to be dependent on local edge velocity and the displacement thickness. The two regions are matched through a continuity of velocity and shear requirement.

Section 3 describes the integral matrix solution procedure which is applied to the governing set of equations. In that section, the splined cubic approximations (achieved through truncated Taylor series expansions) which are used to relate derivatives of the dependent variables are described; the techniques used to evaluate integral terms and streamwise derivatives are given; the Newton-Raphson iteration technique is summarized; and a general description of the matrix solution technique is presented. Results and discussions of typical flow cases are given in Section 4.

SECTION 2

BASIC BOUNDARY LAYER EQUATIONS

2.1 GENERAL EQUATIONS OF MOTION

The equations of motion for a turbulent boundary layer are typically derived from the Navier Stokes equations by decomposition of the velocity field into mean and fluctuating components, time averaging, and making appropriate order of magnitude approximations. Stating the results of these manipulations as a point of departure, the global continuity equation becomes

$$\frac{1}{r_o^k}\frac{\partial \rho u r_o^k}{\partial s} + \frac{\partial \rho v}{\partial y} = 0 \qquad (1)$$

and the momentum equation is

$$\rho u \frac{\partial u}{\partial s} + \rho v \frac{\partial u}{\partial y} = -\frac{dP}{ds} + \frac{\partial}{\partial y}\left(\mu\frac{\partial u}{\partial y} - \overline{\rho u' v'}\right) \qquad (2)$$

Triple correlations and streamwise derivatives of turbulent correlations have been dropped in these equations. The pressure P is the imposed free stream pressure and is related to the free stream velocity through the Bernoulli equation,

$$P + \rho_1 u_1^2/2 = \text{const.} \qquad (3)$$

Equations (1), (2), and (3) would allow calculation of u and v in a constant property boundary layer for the proper boundary and initial conditions if the turbulence term was known. The assumptions made regarding this turbulence term provide the greatest differences between the turbulent boundary-layer techniques available today.

There are many choices available to describe the "Reynolds' stress" term as it appears in equation (2). It would be desirable to write another equation, say a turbulent energy equation, to describe the evolution of the $\overline{\rho u'v'}$ product as the flow progresses downstream, since the momentum equation does not. However, the currently available turbulent energy equation approaches typically involve several constants or special assumptions to achieve a closed set of equations, and would not be readily extendable to compressible, reacting flows. Methods which eliminate the turbulent stress altogether by integrating the momentum equation across the entire boundary layer cannot give the level of detail regarding velocity, temperature, and concentration profiles which is required in a program of this sort. One approach which has met with success for many types of flows is the eddy viscosity description of turbulence. In this approach, the turbulent stress is related to the mean velocity field through the relation

$$\overline{\rho u'v'} = \rho\varepsilon\frac{\partial u}{\partial y} \tag{4}$$

Since this approach lends itself to the more complex systems which will eventually be analyzed with this program, it will be adopted here. The momentum equation becomes

$$\rho u\frac{\partial u}{\partial s} + \rho v\frac{\partial u}{\partial y} = -\frac{dP}{ds} + \frac{\partial}{\partial y}\left[\rho(\varepsilon+\nu)\frac{\partial u}{\partial y}\right] \tag{5}$$

The eddy viscosity ε can be related to global parameters of the flow (δ^*) in the outer portion of the boundary layer, and is typically described by a "law of the wall" in the inner portion of the boundary layer. The procedures adopted for each of these regions are discussed in the following sections.

One other item which deserves some attention in a discussion of the governing equations for turbulent flows is the subject of intermittency. As free stream conditions are approached at the edge of the boundary layer, a zone of turbulent intermittency is encountered in which the turbulent eddies which cause Reynolds stresses occur less and less frequently. This phenomena has been demonstrated to be a result of the irregular free boundary which separates the turbulent and nonturbulent fluid. This intermittency of the turbulent

stresses can be expressed analytically in terms of an intermittency factor, ϕ, which is a measure of the fraction of time the flow is turbulent. Klebanoff (Reference 7) found that for smooth walls, the intermittency factor is closely represented by a Gaussian integral curve centered at 0.78δ, where δ is the local boundary layer thickness. Incorporating the intermittency factor ϕ into the momentum equation, we have

$$\rho u\frac{\partial u}{\partial s} + \rho v\frac{\partial u}{\partial y} = -\frac{dP}{ds} + \frac{\partial}{\partial y}\left[\rho(\phi\varepsilon+\nu)\frac{\partial u}{\partial y}\right] \tag{6}$$

The success of the Gaussian integral curve will be discussed in a later section.

2.2 WALL REGION

2.2.1 One-Dimensional Analysis

The wall region of the turbulent boundary layer is characterized by very steep gradients in the turbulent transport and mean field properties. Turbulent stress varies from zero at the wall to near its maximum value at the outer edge of the wall region. There is a vast amount of empirical evidence that these turbulent stresses and also the mean flow field properties can be described entirely in terms of the wall state, wall fluxes, thermodynamic and transport properties of the fluid, and the normal coordinate y. Since the streamwise coordinate does not enter the solution for this region, the problem becomes a one-dimensional initial value problem. Eliminating x derivatives from the continuity equation results in

$$\frac{d(\rho v)}{dy} = 0 \tag{7}$$

or

$$\rho v = \rho_o v_o \tag{8}$$

where the subscript o refers to the wall value. Thus the wall injection rate, $\rho_o v_o$, which may be a function of x, determines the transverse mass flux

through the entire wall region. Using the same technique for the momentum equation and substituting equation (8),

$$\rho_o v_o u = \rho(\nu+\varepsilon)\frac{du}{dy} - \tau_o \qquad (9)$$

where the wall shear, τ_o, is also typically a function of x. Intermittency, ϕ, has been set to unity for the entire wall region. For flows over an impermeable wall with constant properties, this equation reduces to

$$\rho(\nu+\varepsilon)\frac{du}{dy} = \tau_o \qquad (10)$$

or

$$\tau = \tau_o \qquad (11)$$

indicating that shear can be considered constant in the wall region. For incompressible flows with injection, it is seen that shear varies with the injection rate and local velocity, that is,

$$\tau = \tau_o + \rho_o v_o u \qquad (12)$$

2.2.2 Mixing Length Approximations

A complete investigation of the validity of the mixing length postulate for flows with injection has been reported in Reference 8. The analysis used in this investigation is much the same; therefore, only the basic framework of the analysis will be presented. The reader should refer to Reference 8 for details.

Because of the current lack of understanding of turbulent mechanisms, "theoretical" predictions of the variation of turbulence near the wall must rely on empirical input into relations based on some phenomenological dependence.

Because of the generality of the ultimate goals of this analysis and of the desire to approximate the physical situation, certain prerequisites were established for the turbulent transport relations. These were:

a. The relations must indicate a continuous variation of the turbulent transport properties from the wall to the fully turbulent region.

b. The relations must be generally applicable to mass, momentum, and energy transport.

c. The relations must be extendable to compressible flow with real gas properties.

d. The relations should be suitable for transpired and untranspired boundary layers without any, or a minimum, modification of form.

Two basic types of viscous layer hypotheses have been proposed in the past. The first type predicts the variation of turbulent viscosity from the wall to the fully turbulent regime. Reichardt, Rannie, and Deissler have, in References 9 through 11, for example, proposed such variations. The second type of hypothesis involves a variation of mixing length from the wall into the fully turbulent portion of the boundary layer. Rotta, von Kármán, and Van Driest (References 12 to 14), have adopted this procedure. Data indicate that surface mass addition strongly affects the eddy viscosity profile, and it was found that the first type of hypothesis could not be simply modified to predict this variation. On the other hand, success of the mixing length theory in predicting profiles in the fully turbulent portion of the boundary layer with surface mass addition has been noted, for example, in References 15 and 16. It has generally been concluded that the slope of the linear relation between mixing length and distance from the wall is insensitive to surface mass addition. As a consequence of this apparent generality of the mixing length approach, it was adopted for the present studies.

The basic mixing length postulate can be expressed as

$$-\overline{\rho u'v'} = \rho\ell^2\left(\frac{du}{dy}\right)^2 = \rho\varepsilon\frac{du}{dy} \qquad (13)$$

where the mixing length, ℓ, is a combination of various correlations, but retains some relationship to the scale of turbulence. Prandtl proposed that

this length will, in its simplest form, be related to the distance from a wall, at least in the region of development of turbulence. His proposition that

$$\frac{d\ell}{dy} = \text{constant}, \ K \tag{14}$$

has been tested under a variety of conditions and found to be quite adequate in the fully turbulent portion of the wall regime.

As the wall is approached, however, this simple relation is no longer appropriate and, in fact, it can be shown theoretically that

$$\left.\begin{aligned} &\lim_{y\to 0} \ell = 0 \\ &\lim_{y\to 0} \frac{d\ell}{dy} = 0 \end{aligned}\right\} \tag{15}$$

This is a consequence of the Reichardt-Elrod criterion (see Reference 8). Thus, two criteria are specified, namely, Prandtl's hypothesis which is appropriate in the fully turbulent portion of the wall regime and the Reichardt-Elrod wall criterion as expressed by equation (15).

Several means of expressing a relation covering the full range of y and including these limiting criteria have been used by other investigators. It is advantageous in considering extensions of mixing length theory to establish some physical logic for the selected relation. Unfortunately, the understanding of transition from the laminar to the turbulent portions of the layer has not reached a state permitting any quantitive specification. Therefore, the selected model can be based only on qualitative understanding of the process, dimensional considerations, and the above limiting criteria. These criteria are satisfied by a simple implicit relation of the form

$$\frac{d\ell}{dy} \propto (Ky - \ell) \tag{16}$$

which implies that the rate of increase of the mixing length is proportional to the difference between the value postulated by Prandtl (Ky) and its actual

value. This rate of increase should also be augmented by the local applied shear and retarded by the local viscosity. Using these parameters to non-dimensionalize the above relation yields

$$\frac{d\ell}{dy} = (Ky-\ell) \ \frac{\sqrt{\tau/\rho}}{y_a^+ \nu} \tag{17}$$

where y_a^+ is the constant of proportionality. The coefficients K and y_a^+ were shown in Reference 8 to be invariant for a wide variety of flow conditions at values of 0.44 and 11.83, respectively. For the special case of constant properties and zero injection (constant shear), this equation can be integrated to yield

$$\ell = \frac{K\nu}{u_\tau}\left\{ y^+ - y_a^+ \left[1 - \exp\left(-\frac{y^+}{y_a^+}\right)\right]\right\} \tag{18}$$

where

$$u_\tau = \sqrt{\frac{\tau_o}{\rho}}$$

$$y^+ = \frac{y u_\tau}{\nu}$$

It can be seen that the Reichardt-Elrod criteria is satisfied at the wall and Prandtl's expression is obtained for small y. For large y, Rotta's (Reference 12) expression,

$$\ell = \frac{K\nu}{u_\tau}(y^+ - y_a^+) \tag{19}$$

is obtained. Due to the simplicity and physical adequacy of this model, equation (17) has been adopted for the analysis presented here. Comparisons of this model with data from blowing and no-blowing experiments are given in Reference 8.

2.3 WAKE REGION

The wake region of a turbulent boundary layer is so named because the flow in this region tends to have a wake-like character. In particular, the outer 80 to 90 percent of the boundary layer appears to be a region in which the upstream character of the flow combined with the local turbulent eddies dominate the mixing processes within the flow, and the viscous effects become second order. Gradients in the wake region are typically much smaller than those of the wall region, and intermittency begins to become a factor near the outer edge of the boundary layer. Since the pressure gradient and streamwise derivative terms are important in the wake region, equations (1) and (6) must be solved in their entirety.

A fortunate feature of the wake portion of the boundary layer is that eddy viscosity is nearly constant across this region, at least for equilibrium* incompressible flows. In particular, Clauser (Reference 6) was able to relate the eddy viscosity to edge velocity and a length scale δ^*

$$\epsilon \doteq 0.018\, u_1 \delta^* \qquad (20)$$

for a great quantity of experimental data taken in equilibrium flows. While this empirical evidence cannot be taken as a basic truth for all situations, the expression above has proved accurate and useful for many applications and will be used in this analysis.

Equations (1) and (6) as they stand could indeed be solved by some numerical technique. For the majority of problems, however, it is convenient to transform the problem to a new coordinate system in which the general problem of flow over an arbitrary surface is easier to handle. Also, the transformation may offer the possibility of a "similarity" solution if formulated properly.

*Equilibrium as used here refers to a particular pressure gradient, $(\delta^*/\tau_o)(dP/dx)$, which results in self-similar velocity profiles.

The transformation which was used in the present analysis was arrived at by performing a number of operations on the equations of motion. These included:

a. Combining the two equations by solving the continuity equation for ρv and substituting.

b. Defining a dimensionless stream function f to eliminate the resulting integral term.

c. Utilizing a scaling parameter $\delta(s)$ for y in order to place the equation in dimensionless form. The quantity $\delta(s)$ remains undefined at this point.

d. Rewriting streamwise velocity in terms of the stream function.

e. Defining a new normal coordinate to eliminate density from several terms and to keep the boundary-layer thickness very nearly constant.

f. Defining the constant of integration in the stream function definition to eliminate the wall blowing rate term.

g. Defining a new streamwise coordinate and the y scaling parameter, δ, such that a group of terms becomes constant and the resulting equation is greatly simplified.

Out of this list of operations, steps (c) and (g) are probably least understood. In step (c), it is found that

$$\frac{\partial f}{\partial \bar{y}} = \frac{\rho u}{\rho_1 u_1} \qquad (21)$$

where f is the stream function,

$$f = f_o(s) + \frac{1}{\rho_1 u_1} \int_o^{\bar{y}} \rho u \, d\bar{y} \qquad (22)$$

$\bar{y} = y/\delta$ is the dimensionless y coordinate, and the subscripts o and 1 refer to the wall and boundary layer edge, respectively. It is seen that by a simple transformation,

$$\eta = \alpha(s)\int_0^{\tilde{y}} \frac{\rho}{\rho_1}\, d\tilde{y} \tag{23}$$

density can be eliminated from the stream function equation, that is,

$$\frac{\partial f}{\partial \eta} = \frac{f'}{\alpha(s)} = u/u_1. \tag{24}$$

and also from several terms in the momentum equation. The $\alpha(s)$ paramoter is a stretching parameter in the normal direction whose purpose is to keep the boundary-layer thickness relatively constant. The advantage of this, of course, is that a "universally applicable" nodal network can be chosen a priori. A procedure which has worked well is to choose a value of α such that a nodal point near the boundary layer edge, η_c, has a specified streamwise velocity associated with it, near but not equal to the edge velocity:

$$\frac{f'\big|_{\eta_c}}{\alpha} = \frac{C\, f'\big|_{\eta_e}}{\alpha} = C \tag{25}$$

or

$$\alpha = \frac{f'\big|_{\eta_c}}{C} \tag{26}$$

The transformation involving α is discussed further in Reference 17.

Step (g) in the list of operations is perhaps the most interesting in that it differentiates the turbulent transformation from a laminar one. Steps (a) through (f) result in the differential equation

$$f'\frac{\partial f'}{\partial(\ln s)} - f'\,\frac{d(\ln \alpha)}{d(\ln s)} - f''\frac{\partial f}{\partial(\ln s)} = \frac{s}{\alpha\delta}\,\frac{\partial}{\partial\eta}\left[\left(\frac{\rho}{\rho_1}\right)^2\left(\frac{\varepsilon+\nu}{u_1\delta}\right)f''\right]$$
$$+\frac{d(\ln u_1)}{d(\ln s)}\left(\frac{\rho_1}{\rho}\,\alpha^2 - f'^2\right) + ff''\,\frac{d\left[\ln(\rho_1 u_1 r_o^K \delta\,]\right.}{d(\ln s)} \tag{27}$$

The objective in step (g) is to define the y scaling parameter δ and also a new streamwise coordinate ξ such that the coefficients of the first and last terms on the right-hand side of the equation become constant. This can be done if one defines

$$\xi = \int_0^s \rho_1 u_1 r_o^K\, ds \tag{28}$$

$$\delta = \frac{\xi}{\rho_1 u_1 r_o^K} \tag{29}$$

The momentum equation becomes

$$ff'' + \frac{1}{\alpha}\left[\left(\frac{\rho}{\rho_1}\right)^2\left(\frac{\varepsilon+\nu}{u_1\delta}\right)f''\right]' + \frac{\beta}{2}\left(\frac{\rho_1}{\rho}\,\alpha^2 - f'^2\right)$$
$$= \alpha f'\,\frac{\partial(f'/\alpha)}{\partial(\ln \xi)} - f''\,\frac{\partial f}{\partial(\ln \xi)} \tag{30}$$

where

$$\beta \quad \frac{2\,d(\ln u_1)}{d(\ln \xi)}$$

Note that δ in this transformation is a linear function of running length, similar to the growth of a turbulent boundary layer. The δ appearing in the second term was left in the problem in order to form the Clauser parameter, $\frac{\varepsilon}{u_1\delta^*}$, which is taken as constant:

$$ff'' + \frac{1}{\alpha}\left[\left(\frac{\rho}{\rho_1}\right)^2\left(\frac{\varepsilon}{u_1\delta^*}\right)\left(\frac{\delta^*}{\delta}\right)f''\right]' + \frac{\beta}{2}\left(\frac{\rho_1}{\rho}\,\alpha^2 - f'^2\right)$$
$$= \alpha f'\,\frac{\partial(f'/\alpha)}{\partial(\ln \xi)} - f''\,\frac{\partial f}{\partial(\ln \xi)} \tag{31}$$

Kinematic viscosity has been dropped for the purposes of this explanation. For laminar flow, the δ under the brackets in equation (27) would have been brought outside, resulting in

$$\delta = \frac{\xi^{\frac{1}{2}}}{\rho_1 u_1 r_o^{\kappa}} \tag{32}$$

which gives the conventional Levy-Lees transformation.

Summarizing the transformations which are used,

$$\left.\begin{aligned} \xi &= \int_0^s \rho_1 u_1 r_o^{\kappa} ds \\ \eta &= \frac{1}{\delta a}\int \frac{\rho}{\rho_1} dy \\ \zeta &= \frac{\xi}{\rho_1 u_1 r_o^{\kappa}} \\ f &= f_o + \frac{1}{\rho_1 u_1 \delta} \int_0^y \rho u dy \\ f_o &= -\frac{1}{\rho_1 u_1 \delta r_o^{\kappa}} \int_0^s \rho_o v_o r_o^{\kappa} ds \end{aligned}\right\} \tag{33}$$

The simplifications for constant density flow are obvious. For this special case, the governing momentum equation becomes

$$ff'' + \frac{1}{a}\left[\left(\frac{\varepsilon+\nu}{u_1\delta}\right) f''\right]' + \frac{\beta}{2}(a^2 - f'^2)$$

$$= af' \frac{\partial\left(f'/a\right)}{\partial\left(\ln \xi\right)} - f'' \frac{\partial f}{\partial(\ln \zeta)} \tag{34}$$

and the mixing length equation is

$$\ell' - \left(\frac{K\eta\delta a - \ell}{y_a^+}\right)\left[Re_\delta \left(1 + \frac{\varepsilon}{\nu}\right) f''\right]^{\frac{1}{2}} = 0 \tag{35}$$

2.4 MATCHING OF THE WALL AND WAKE SOLUTIONS

Two eddy viscosities have been mentioned in the previous sections, namely

$$\varepsilon_1 = \ell^2 \frac{du}{dy} \tag{13}$$

in the wall region and

$$\varepsilon_2 = 0.018\, u_1 \delta^* \tag{20}$$

in the wake. Assuming these equations are accurate descriptions of the physical situation, it is expected that ε_1 would increase with distance away from the wall (beginning at zero) until its value surpassed that of ε_2, at which point ε_2 would be the governing value. This situation is shown schematically below.

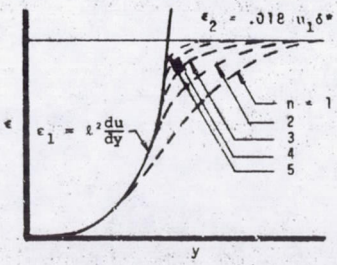

In the present solution procedure, both ε_1 and ε_2 are evaluated at every nodal point in the boundary layer and the two values are combined by the relation

$$\varepsilon = \frac{\varepsilon_1 \varepsilon_2}{\left(\varepsilon_1^{\,n} + \varepsilon_2^{\,m}\right)^{1/n}} \tag{36}$$

Note that this expression results in the smaller of the two eddy viscosities when the two values are grossly different in magnitude, and results in a smooth transition from one expression to the other when the two numbers are of the same order. The schematic above shows the effect of different values for n_i at present a value of five is being used; however, this is easily changed on the program data cards.

2.5 COMMENTS REGARDING TRANSITION

The flow model as presented above has been developed strictly for turbulent flows. Laminar flow problems can also be analyzed; however, similar solutions in the laminar regime will be incorrect due to the nature of the coordinate transformation. An interesting feature of the equations as formulated above is that transition from laminar to turbulent flow is effected automatically. At low Reynolds numbers, $\frac{\varepsilon}{\nu} << 1$ and the eddy viscosity contribution to the solution is negligible. For large Reynolds numbers, ε dominates the shear term, resulting in turbulent profiles. It is apparent that premature transition is obtained if the Clauser parameter is left at 0.018 for the laminar and transitional phases of the flow, since $\frac{\varepsilon}{\nu} = 1.0$ when $Re_{\delta^*} \equiv u_1\delta^*/\nu$ is only 56. A means for describing the rate of approach of ε to its "equilibrium" value of $0.018\, u_1\delta^*$ would thus be required to depict transition more accurately.

SECTION 3

INTEGRAL MATRIX SOLUTION PROCEDURE

The solution of the transformed boundary-layer equations presented in Section 2 utilizes an integral matrix method which has been developed specifically for the solution of chemically reacting, nonsimilar, coupled boundary layers (see Reference 17). In this procedure, the dependent variable f' and its derivatives with respect to η are related by truncated Taylor series expansions such that f' is represented by connected cubics with continuous first and second derivatives at the junction points (commonly called a spline fit). Primarily for convenience, the momentum equation is integrated using a weighting function which is unity between adjacent nodal points and zero elsewhere. The linear Taylor series expansions together with linear boundary conditions form a very sparse matrix which has to be inverted only once for a given problem. The mixing length equation solution can be found immediately in terms of Dawson integral functions. The nonlinear boundary layer equations and the nonlinear boundary conditions are then solved by a Newton-Raphson iteration technique.

In Section 3.1, the Taylor series expansions are presented. The boundary layer equations are integrated, and the integrals which appear are also expanded in Taylor series. The resulting equations are precisely those which have been programmed for solution on high-speed digital computers to represent the incompressible boundary layer with blowing or suction. In Section 3.2, the method of solution for the mixing length equation is presented. The procedure utilized for solving the sets of linear and nonlinear algebraic equations developed in Section 3.1 is then presented in Section 3.3.

3.1 INTEGRAL STRIP EQUATIONS WITH SPLINE INTERPOLATION FUNCTIONS

Consider the boundary layer in the region of a given streamwise station s as being divided into N-1 strips connecting N nodal points. These nodal points are designated by η_i where i = 1 at the wall and N at the edge of the boundary layer.

Consider a function p(y) which with all its derivatives is continuous in the neighborhood of the point y = a. Then, for any value of y in this neighborhood, p(y) may be expressed in a Taylor series expansion as

$$p(y) = p(a) + \frac{p'(a)}{1!}(y-a) + \frac{p''(a)}{2!}(y-a)^2 + \frac{p'''(a)}{3!}(y-a)^3 + \frac{p''''(a)}{4!}(y-a)^4 + \ldots \quad (37)$$

Considering the point a as η_i and the y as η_{i+1}

$$p_{i+1} = p_i + p_i'\delta\eta + p_i''\frac{(\delta\eta)^2}{2} + p_i'''\frac{(\delta\eta)^3}{6} + p_i''''\frac{(\delta\eta)^4}{24} + \ldots \quad (38)$$

where

$$\delta\eta = \eta_{i+1} - \eta_i \quad (39)$$

Conventional finite difference schemes, in effect, typically truncate the Taylor series after the first term and use the resulting expression to relate p' to p, etc., that is,

$$p_i' = \frac{p_{i+1} - p_i}{\delta\eta} \quad (40)$$

Round-off error is then of order $(\delta\eta)^2$ and many nodes must be chosen to bring this value down to acceptable limits. One can achieve a reduction in the number of nodes for a given accuracy by employing a cubic relation representing the function p over the interval of interest. This can be achieved by truncating the Taylor series after the fourth term. Since the third derivative of a cubic is constant over the interval, one can write

$$p_{i+1}''' = \frac{p_{i+1}'' - p_i''}{\delta\eta} \quad (41)$$

Using this in the Taylor series yields

$$-p_{i+1} + p_i + p_i'\delta\eta + p_i''\frac{(\delta\eta)^2}{3} + p_{i+1}''\frac{(\delta\eta)^2}{6} = 0 \quad (42)$$

Similar expressions can be written starting with higher or lower derivatives. For the problem at hand, the following equations can be written relating the dependent variables and their derivatives:

$$f_{n+1} = f_n + f_n'\delta\eta + f_n''\left[\frac{(\delta\eta)^2}{2}\right] + f_n'''\left[\frac{(\delta\eta)^3}{8}\right] + f_{n+1}'''\left[\frac{(\delta\eta)^3}{24}\right] \quad (43)$$

$$f_{n+1}' = f_n' + f_n''\delta\eta + f_n'''\left[\frac{(\delta\eta)^2}{3}\right] + f_{n+1}'''\left[\frac{(\delta\eta)^2}{6}\right] \quad (44)$$

$$f_{n+1}'' = f_n'' + f_n'''\frac{\delta\eta}{2} + f_{n+1}'''\frac{\delta\eta}{2} \quad (45)$$

Notice that f' has been taken to be a cubic over each strip, rather than the stream function, f, since it was desired to represent velocity ($u = u_1 f'/a$) with the cubic. Equations (43) through (45) above, when written for each adjacent pair of nodes, give 3N-3 simultaneous algebraic equations for the 4N+1 unknowns, f_n, f_n', f_n'', f_n''', a, at each streamwise station.* Additional relations must come from the governing differential equations and the boundary

*The mixing length equation (17) is not included in this equation count since mixing length (as well as ϵ in the wake region) is treated as a state property.

conditions. It is important to note that the f, f', etc., are treated as independent variables related by algebraic equations. It is also important to note that the coefficients in equations (43) through (45) are functions of ξ only; therefore, this portion of the resulting matrix need be inverted only once for a given problem.

The momentum equation in the form of equation (34) contains streamwise derivative or "nonsimilar" terms. In the present solution technique, two or three point finite difference formulas are used to express these derivatives. As in Reference 17,

$$\left[\frac{d(\ )}{d(\ln \xi)}\right]_i = d_0(\ )_i + d_1(\ )_{i-1} + d_2(\ )_{i-2} \tag{46}$$

where $(\ )_{i-1}$ refers to the previous streamwise station, and

$$d_0 = \frac{1}{\xi^{\Delta}_{i-1}}, \quad d_1 = -\frac{1}{\xi^{\Delta}_{i-1}}, \quad d_2 = 0 \tag{47}$$

for two-point difference and

$$\left.\begin{aligned} d_0 &= \frac{\xi^{\Delta}_{i-1} + \xi^{\Delta}_{i-2}}{\xi^{\Delta}_{i-1}\,\xi^{\Delta}_{i-2}}, \quad d_1 = \frac{\xi^{\Delta}_{i-2}}{\xi^{\Delta}_{i-1}\,\xi^{\Delta}_{i-1}\,\xi^{\Delta}_{i-2}}, \\ d_2 &= \frac{\xi^{\Delta}_{i-1}}{\xi^{\Delta}_{i-2}\,\xi^{\Delta}_{i-1}\,\xi^{\Delta}_{i-2}} \end{aligned}\right\} \tag{48}$$

for three-point difference where typically

$$\xi^{\Delta}_{i-1} = \ln \xi_i - \ln \xi_{i-1} = \ln (\xi_i/\xi_{i-1}) \tag{49}$$

The three-point difference relation is utilized unless a similar solution is desired (in which case $d_0 = d_1 = d_2 = 0$) or unless the point in question is the first point after either (1) a similar solution or (2) a discontinuity (e.g., where the body changes shape abruptly, or where mass injection is suddenly terminated).

Utilizing these expressions, the momentum equation becomes

$$(1+d_o)\, ff'' + \frac{1}{\alpha}\left[\frac{f''}{Re_\delta} + \frac{\delta^*}{\delta}\frac{\varepsilon}{u_1\delta^*}\phi f''\right]' + \frac{\beta}{2}\alpha^2 - \left(\frac{\beta}{2} + d_o\right) f'^2$$

$$= f'\alpha\left[d_1\left(\frac{f'}{\alpha}\right)_{i-1} + d_2\left(\frac{f'}{\alpha}\right)_{i-2}\right] - f''(d_1 f_{i-1} + d_2 f_{i-2}) \tag{50}$$

This equation is now integrated across each strip in the boundary layer. The solution can actually proceed very nicely without integrating across the strips (see Reference 18) without any noticeable change in speed, accuracy, or stability. However, in multicomponent boundary-layer problems, the resulting relations are greatly simplified by this operation. Integrating from i-1 to i,

$$\left[(1 + d_o) ff'\right]_{i-1}^{i} - \int_{i-1}^{i} (1 + d_o)\, f'^2 d\eta + \frac{1}{\alpha}\left[\frac{f''}{Re_\delta}\right.$$

$$\left. + \frac{\delta^*}{\delta}\frac{\varepsilon}{u_1\delta^*}\phi f''\right]_{i-1}^{i} + \frac{\beta}{2}\alpha^2 (\eta_i - \eta_{i-1}) - \left(\frac{\beta}{2} + d_o\right)\int_{i-1}^{i} f'^2 d\eta$$

$$= \int_{i-1}^{i} f'\alpha\left[d_1\left(\frac{f'}{\alpha}\right)_{i-1} + d_2\left(\frac{f'}{\alpha}\right)_{i-2}\right] d\eta - \int_{i-1}^{i} f''(d_1 f_{i-1}$$

$$+ d_2 f_{i-2})\, d\eta \tag{51}$$

or,

$$\left[(1+d_o)ff\right]_{i-1}^{i} - \int_{i-1}^{i}(1+d_o)f'^2 d\eta + \frac{1}{\alpha}\left[\frac{f''}{Re_\delta} + \frac{\delta^*}{\delta}\frac{\varepsilon}{u_1\delta^*}\phi f'\right]_{i-1}^{i}$$

$$+ \frac{\beta}{2}\alpha^2(\eta_i-\eta_{i-1}) - \left(\frac{\beta}{2}+d_o\right)\int_{i-1}^{i} f'^2 d\eta = \int_{i-1}^{i} f'\left(d_1 f'_{i-1}\right.$$

$$\left. + d_2 f'_{i-2}\right)d\eta + \alpha\int_{i-1}^{i} f'\left[d_1\left(\frac{f'}{\alpha}\right)_{i-1} + d_2\left(\frac{f'}{\alpha}\right)_{i-2}\right]d\eta$$

$$- \left[f'\left(d_1 f_{i-1} + d_2 f_{i-2}\right)\right]_{i-1}^{i} \qquad (52)$$

The Taylor series approximations introduced earlier can also be used to express the integral terms above. Taking $\int_{i-1}^{i} f'p\, d\eta$ as an example, suppose

$$\int f'p\, d\eta = G(\eta) \qquad (53)$$

Then

$$\int_{i-1}^{i} f'p\, d\eta = G(\eta_i) - G(\eta_{i-1}) \qquad (54)$$

Expressing $G(\eta_{i-1})$ in a Taylor series about η_i,

$$G(\eta_{i-1}) = G(\eta_i) + G'(\eta_i)(-\delta\eta) - G''(\eta_i)\frac{(-\delta\eta)^2}{2!} + \ldots \qquad (55)$$

Then

$$\int_{i-1}^{i} f'p\, d\eta = G(\eta_i) - G(\eta_i) - G'(\eta_i)(-\delta\eta) - G''(\eta_i)\frac{(-\delta\eta)^2}{2!} - \ldots \qquad (56)$$

$$= f'_i p_i \frac{\delta\eta}{1!} - (f'_i p'_i + f''_i p_i)\frac{(\delta\eta)^2}{2!}$$

$$+ (f'_i p''_i + 2f''_i p'_i + f'''_i p_i)\frac{(\delta\eta)^3}{3!}$$

$$- (f'_i p'''_i + 3f''_i p''_i + 3f'''_i p'_i + f''''_i p_i)\frac{(\delta\eta)^4}{4!}$$

$$+ (4f'_i p'''_i + 6f''_i p''_i + 4f''''_i p'_i)\frac{(\delta\eta)^5}{5!}$$

$$- (10f''_i p'''_i + 10f''''_i p''_i)\frac{(\delta\eta)^6}{6!}$$

$$+ 20f''''_i p''_i \frac{(\delta\eta)^7}{7!} + \ldots \qquad (57)$$

where, consistent with the truncation of the Taylor series employed earlier, all derivatives greater than f_i''' and p_i'' have been dropped. Utilizing again equations (41) to eliminate p_i''', equation (57) becomes

$$\int_{i-1}^{i} f'p\, d\eta = f'_i XP_1 + f''_i XP_2 + f'''_i XP_3 + f'''_{i-1} XP_4 \qquad (58)$$

where

$$XP_1 = \delta\eta\left(p_i - p'_i\frac{\delta\eta}{2} + p''_i\frac{(\delta\eta)^2}{8} + p''_{i-1}\frac{(\delta\eta)^2}{24}\right)$$

$$XP_2 = -\delta\eta^2\left(\frac{p_i}{2} - p'_i\frac{\delta\eta}{3} + p''_i\frac{11(\delta\eta)^2}{120} + p''_{i-1}\frac{(\delta\eta)^2}{30}\right)$$

$$XP_3 = \delta\eta^3\left(\frac{p_i}{8} - p'_i\frac{11\delta\eta}{120} + p''_i\frac{11(\delta\eta)^2}{420} + p''_{i-1}\frac{5(\delta\eta)^2}{504}\right)$$

$$XP_4 = \delta\eta^3\left(\frac{p_i}{24} - p'_i\frac{\delta\eta}{30} + p''_i\frac{5(\delta\eta)^2}{504} + p''_{i-1}\frac{(\delta\eta)^2}{252}\right) \qquad (59)$$

Similar operations were carried out for the integral terms appearing in equation (52) above, resulting in the relation

$$\left[(1+d_o)ff'\right]_{i-1}^{i} + \frac{1}{\alpha}\left[\frac{f''}{Re_\delta} + \left(\frac{\delta^*}{\delta}\right)\left(\frac{\varepsilon}{u_1\delta^*}\right) + f''\right]_{i-1}^{i} + \frac{\beta}{2}\alpha^2(\eta_i - \eta_{i-1})$$

$$- \left(1+2d_o+\frac{\beta}{2}\right)\left[f_n'X_1 + f_n''X_2 + f_n'''X_3 + f_{n-1}'''X_4\right] - \left[f_n'Z_1 + f_n''Z_2\right.$$

$$\left. + f_n'''Z_3 + f_{n-1}'''Z_4\right] - \alpha\left[f_n'ZA_1 + f_n''ZA_2 + f_n'''ZA_3 + f_{n-1}'''ZA_4\right]$$

$$+ \left[f'\left(d_1 f_{\ell-1} + d_2 f_{\ell-2}\right)\right]_{i-1}^{i} = 0 \qquad (60)$$

where in the X functions, $p = f'$, in the Z functions, $p = d_1 f'_{\ell-1} + d_2 f'_{\ell-2}$, and in the ZA functions, $p = d_1\left(\frac{f'}{\alpha}\right)_{\ell-1} + d_2\left(\frac{f'}{\alpha}\right)_{\ell-2}$. Equation (60) above provides N-1 more relations between the 4N+1 variables. The definition of α and the boundary conditions supply the additional relations.

The definition of α was given in equation (26). For each problem, a node is chosen near the edge of the boundary layer and the velocity ratio $u/u_1 = 0.99$ (or some other number near 1.0) is specified there. The stretching parameter α is then defined by the relation

$$\alpha = \frac{f'}{0.99} \quad @ \text{ that node} \qquad (61)$$

The boundary conditions are as follows:

$$\left.\begin{aligned} f_1 &= f_o \\ f_1' &= 0 \end{aligned}\right\} \qquad (62)$$

At the edge of the boundary layer*

$$\left.\begin{aligned} f' &= \alpha \\ f'' &= 0 \end{aligned}\right\} \qquad (63)$$

Thus, we have 4N+1 equations for the 4N+1 unknowns. These equations are solved by a Newton-Raphson iteration technique explained in Section 3.3.

3.2 SOLUTION OF THE MIXING LENGTH EQUATION

The mixing length equation is a first order linear differential equation whose solution can be written directly in general terms. The differential equation is

$$\frac{d\ell}{dy} = (Ky-\ell)\frac{\sqrt{\tau_o/\rho}}{y_a^+\nu} \qquad (17)$$

Defining

$$P(y) = \frac{\sqrt{\tau_o/\rho}}{y_a^+\nu} \qquad (64)$$

results in

$$\frac{d\ell}{dy} + P\ell = KPy \qquad (65)$$

The solution to this equation is

$$\ell = K\left[y - \frac{\int_o^y e^{\int_o^{y'} P dy''} dy'}{\int_o^y P dy'}\right] \qquad (66)$$

*The second edge boundary condition is not usually imposed in the boundary-layer problem, but is obtained from the solution. The need for this condition is a direct result of the use of cubic spline fits. The requirement for it vanishes with the use of quadratic spline fits.

The remaining problem is to evaluate the integral terms. Defining

$$L = \frac{\int_0^y e^{\int_0^{y'} P dy''} dy'}{\int_0^y P dy'} \tag{67}$$

yields

$$\ell = K(y-L) \tag{68}$$

Evaluating L at the i^{th} node, it can be shown that

$$L_i = \frac{L_{i-1}}{\int_{y_{i-1}}^{y_i} P dy'} e^{\int_0^{\Delta_i} P dy} + \frac{\int_0^{\Delta_i} e^{\int_0^y P dy'} dy}{\int_0^{\Delta_i} P dy} \tag{69}$$

where y in the right-hand integral term has the bottom edge of the strip as its origin and

$$\Delta_i = y_i - y_{i-1} \tag{70}$$

Assuming a linear variation of P(y) across the strip gives

$$L_i = \frac{L_{i-1}}{\frac{P_i + P_{i-1}}{2}\Delta_i} e^{\int_0^{\Delta_i} e^{-\left[(a\Delta_i + c)^2 - (ay+c)^2\right]} dy} \tag{71}$$

where $a = \frac{P_i - P_{i-1}}{2\Delta_i}$

$c = \frac{P_{i-1}}{2a}$

By redefining variables

$$\tilde{y} = ay + c, \qquad d = a\Delta_i + c$$

one obtains

$$L_i = \frac{L_{i-1}}{\frac{P_i + P_{i-1}}{2}\Delta_i} e^{\frac{1}{a}\left[e^{-d^2}\int_0^d e^{\tilde{y}^2} d\tilde{y} - \frac{e^{-d^2}e^{-c^2}}{e^{-c^2}}\int_0^c e^{\tilde{y}^2} d\tilde{y}\right]} \tag{72}$$

$$L_i = \frac{L_{i-1}}{\frac{P_i + P_{i-1}}{2}\Delta_i} e^{\frac{1}{a}\left[D(d) - e^{(c^2-d^2)}D(c)\right]} \tag{73}$$

where

D( ) = the Dawson integral* of the quantity in brackets.

The Dawson integral can be evaluated from tables (Reference 19) or by a series method. In any case, an explicit recursion formula for the mixing length solution at each node has been arrived at.

3.3 SOLUTION OF THE BOUNDARY LAYER EQUATIONS

The solution of the boundary-layer equations presented in Section 3.1 is accomplished by general Newton-Raphson iteration. In this section these equations are put into a form suitable for solution by the Newton-Raphson procedure.

---

*$D(x) = e^{-x^2}\int_0^x e^{y^2} dy$

The resulting equations are then written in matrix form, and a method is presented for their solution. The procedure attempts to minimize computational time and computer storage requirements.

In order to illustrate the Newton-Raphson method consider two simultaneous nonlinear algebraic equations

$$F(x,y) = 0 \qquad G(x,y) = 0 \tag{74}$$

the solution for which is given by $x = \bar{x}$, $y = \bar{y}$. Define x_m and y_m as the values of x and y for the m^{th} iteration. The desired solution $f(\bar{x},\bar{y})$ can be expressed in a Taylor series expansion

$$\left.\begin{aligned} 0 = F(\bar{x},\bar{y}) &= F(x_m, y_m) + (\bar{x} - x_m)\,\frac{\partial F(x_m,y_m)}{\partial x} \\ &\quad + (\bar{y} - y_m)\,\frac{\partial F(x_m,y_m)}{\partial y} + \cdots \\ 0 = G(\bar{x},\bar{y}) &= G(x_m,y_m) + (\bar{x} - x_m)\,\frac{\partial G(x_m,y_m)}{\partial x} \\ &\quad + (\bar{y} - y_m)\,\frac{\partial G(x_m,y_m)}{\partial y} + \cdots \end{aligned}\right\} \tag{75}$$

The Newton-Raphson method consists of replacing $(\bar{x},\bar{y})$ by (x_{m+1}, y_{m+1}) on the right-hand side of these expressions and neglecting nonlinear terms in $x_{m+1} - x_m$ and $y_{m+1} - y_m$. This yields the set of simultaneous equations

$$\left.\begin{aligned} \Delta x_m \frac{\partial F(x_m,y_m)}{\partial x} + \Delta y_m \frac{\partial F(x_m,y_m)}{\partial y} &= -F(x_m,y_m) \\ \Delta x_m \frac{\partial G(x_m,y_m)}{\partial x} + \Delta y_m \frac{\partial G(x_m,y_m)}{\partial y} &= -G(x_m,y_m) \end{aligned}\right\} \tag{76}$$

or, in matrix form

$$\begin{bmatrix} \frac{\partial F(x_m,y_m)}{\partial x} & \frac{\partial F(x_m,y_m)}{\partial y} \\ \frac{\partial G(x_m,y_m)}{\partial x} & \frac{\partial G(x_m,y_m)}{\partial y} \end{bmatrix} \begin{bmatrix} \Delta x_m \\ \Delta y_m \end{bmatrix} = \begin{bmatrix} -F(x_m,y_m) \\ -G(x_m,y_m) \end{bmatrix} \tag{77}$$

where

$$\Delta x_m \equiv x_{m+1} - x_m \qquad \Delta y_m \equiv y_{m+1} - y_m \tag{78}$$

The Δx_m and Δy_m are the corrections to be added to x_m and y_m, respectively, to yield the values of the dependent variables for the $m+1^{th}$ iteration. Here $F(x_m,y_m)$ and $G(x_m,y_m)$ are the values of the original functions $F(x,y)$ and $G(x,y)$ evaluated for $x = x_m$ and $y = y_m$. As the corrections approach zero, the $F(x_m,y_m)$ and $G(x_m,y_m)$ thus approach zero. Hence, it is appropriate to look upon these as errors associated with the original equation (74). It is apparent that this procedure can be extended to an arbitrary number of functions and a corresponding number of primary variables.

For the problem at hand, partial derivatives of each governing equation or boundary condition equation are found with respect to each of the variables f, f', f'', f''', and α. A matrix of these coefficients is then formed, similar to the 2x2 matrix above, and a solution for the corrections is found. The corrections to the dependent variables are made and the errors in each equation are calculated. If these errors are not within some acceptable value, a new matrix of coefficients is formed, new corrections calculated, and so on.

The process described above sounds very time-consuming for a typical situation in which, say, 10 nodes are used in the boundary layer. This would require the inversion of a 41x41 matrix plus the recalculation of the coefficients on every iteration. Fortunately, the coefficient matrix is very sparsely populated and lends itself to a very high-speed inversion process; therefore, computation time is short.

The biggest time-saving factor is the fact that the Taylor series equations, which account for more than half of the matrix, have coefficients which are functions of the node spacing only. Thus, explicit relations for the corrections in JN-3 of the variables in terms of the other N+4 variables may be found once the node spacing is selected. The remaining terms of the coefficient matrix change with each iteration. However, since a great many of the coefficients are zero, special routines have been written to load and invert the array on each iteration. Typically, three to six iterations are required to reach a satisfactory solution.

SECTION 4

RESULTS AND DISCUSSION

4.1 EFFECT OF INCLUDING INTERMITTENCY

As discussed earlier, the turbulent intermittency was included in the momentum equation (6). The effects of including an intermittency expression for the flat plate flow of Reference 20 were examined and are presented here. Using the Gaussian integral curve centered at 0.78δ, the expression for intermittency is

$$\phi = 0.5 \left[1 - \text{erf}\ (5.05\ \frac{y}{\delta} - 3.95)\right]$$

Boundary layer thickness δ was taken as that point where $u/u_1 = 0.99$. Figure 1 illustrates the resulting velocity profiles.

Very poor agreement was obtained with this choice for δ, which demonstrates the major problem in utilizing the suggested intermittency curve -- the definition of δ. When the intermittency curve was shifted out 25 percent (i.e., centered at $y/\delta = .98$), the effect of intermittency nearly disappeared. For this particular station, the best agreement in profile shape was obtained by removing intermittency altogether ($\phi = 1.0$ everywhere). This being the case, the remaining predictions presented in this report were made without considering the intermittency.

4.2 FLOWS OVER IMPERMEABLE WALLS

Figures 2 through 6 demonstrate the utility of the program for flows over impermeable walls. The integral parameters C_f, Re_θ, and H are presented for each of four flows in Figures 2 through 5, and typical velocity profiles are presented in Figure 6. In Figure 2, the predictions for a flat plate flow with no pressure gradient are compared with the experimental data of Reference 20.

The biggest time-saving factor is the fact that the Taylor series equations, which account for more than half of the matrix, have coefficients which are functions of the node spacing only. Thus, explicit relations for the corrections in 3N-3 of the variables in terms of the other N+4 variables may be found once the node spacing is selected. The remaining terms of the coefficient matrix change with each iteration. However, since a great many of the coefficients are zero, special routines have been written to load and invert the array on each iteration. Typically, three to six iterations are required to reach a satisfactory solution.

SECTION 4

RESULTS AND DISCUSSION

4.1 EFFECT OF INCLUDING INTERMITTENCY

As discussed earlier, the turbulent intermittency was included in the momentum equation (6). The effects of including an intermittency expression for the flat plate flow of Reference 20 were examined and are presented here. Using the Gaussian integral curve centered at 0.78δ, the expression for intermittency is

$$\phi = 0.5 \left[1 - \text{erf}\ (5.05\ \frac{Y}{\delta} - 3.95)\right]$$

Boundary layer thickness δ was taken as that point where $u/u_1 = 0.99$. Figure 1 illustrates the resulting velocity profiles.

Very poor agreement was obtained with this choice for δ, which demonstrates the major problem in utilizing the suggested intermittency curve -- the definition of δ. When the intermittency curve was shifted out 25 percent (i.e., centered at $y/\delta = .98$), the effect of intermittency nearly disappeared. For this particular station, the best agreement in profile shape was obtained by removing intermittency altogether ($\phi = 1.0$ everywhere). This being the case, the remaining predictions presented in this report were made without considering the intermittency.

4.2 FLOWS OVER IMPERMEABLE WALLS

Figures 2 through 6 demonstrate the utility of the program for flows over impermeable walls. The integral parameters C_f, Re_θ, and H are presented for each of four flows in Figures 2 through 5, and typical velocity profiles are presented in Figure 6. In Figure 2, the predictions for a flat plate flow with no pressure gradient are compared with the experimental data of Reference 20.

The measured velocity profile at X = 0.387 meters was used as the starting condition. Results are seen to be excellent at all stations, as might be expected because of the simplicity of the problem.

Figure 3 includes comparisons of predictions with the accelerating flow data of Reference 22. Drag coefficient and form factor predictions are again in excellant agreement with the data, maximum errors being less than 5 percent. Reynolds number based on θ is consistently high; however, the error is less than 10 percent. Figure 4 contains data and prediction comparisons for a decelerating flow, Reference 23. Predictions were made only for the four stations at which experimental data were obtained, using the first station as an initial condition. No investigation of the effect of including intermediate stations between experimental data points was made; however, this approach may result in improved agreement. For the straightforward approach used, agreement is excellent for H and Re_θ and errors are less than 10 percent for C_f. The final impermeable wall test case is presented in Figure 5. These data were obtained for a flow which negotiates a strong pressure rise, then "relaxes" in a constant pressure region downstream. This highly nonequilibrium (in the fluid mechanical rather than chemical sense) situation provides perhaps the most strenuous test of the eddy viscosity model being used because of the model's complete dependence on the displacement thickness δ^*. For a flow such as this one, δ^* would be expected to change much faster than the turbulence level. The ability of the program to predict the unusual variations in C_f and Re_θ is amazingly good, however. It should be kept in mind that the drag coefficients for all the impermeable wall cases were calculated in Reference 21 by assuming the validity of a law of the wall, a procedure which breaks down to some extent for flows with very strong adverse pressure gradients. A check on the accuracy of C_f was also provided in Reference 21 by summing the various terms in the integral momentum equation. For strong pressure gradient cases such as this one, there was a significant error indicated by the failure of the integral momentum equation to be satisfied. Thus, some of the error indicated in Figure 5 may be in the data as well as the prediction. Typical velocity profiles for two of the cases presented earlier are shown in Figure 6. Agreement is again seen to be excellent.

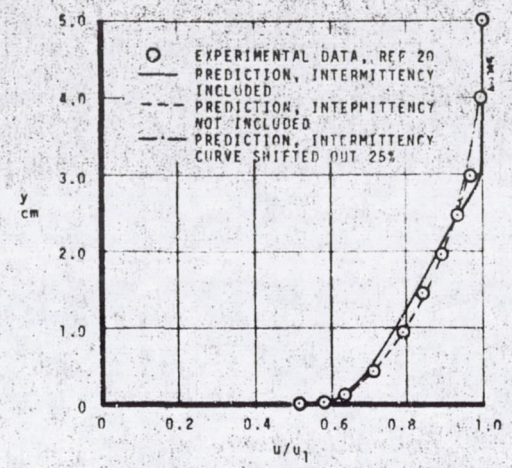

Figure 1. Velocity Profiles with Intermittency Included (Flat Plate Flow with No Blowing, S = 2.537 Meters)

4.3 FLOWS WITH BLOWING

The real test of a turbulent boundary layer program of this sort is its performance for flows with strong blowing. For this type of flow, the shear stress in the one-dimensional wall region must be treated as a variable (equation (17)), which introduces potential stability problems into the solution of the mixing length equation. The results for the solution technique presented in this report are very encouraging, however. Figure 7 shows a drag coefficient prediction for some strong blowing data from Reference 16. The solution was started by allowing a similar solution at S = 1.00 inches (no streamwise derivative terms) with blowing, and marching on downstream with nonsimilar solutions from that point. It is unclear in many cases how blowing solutions should be compared to experimental data where boundary layer trips and unblown initial portions of the surface may affect the profiles. The predictions shown in Figure 7 are compared on the basis of the same S-station. The drag coefficient appears to be correct to within the accuracy of the data; however, a

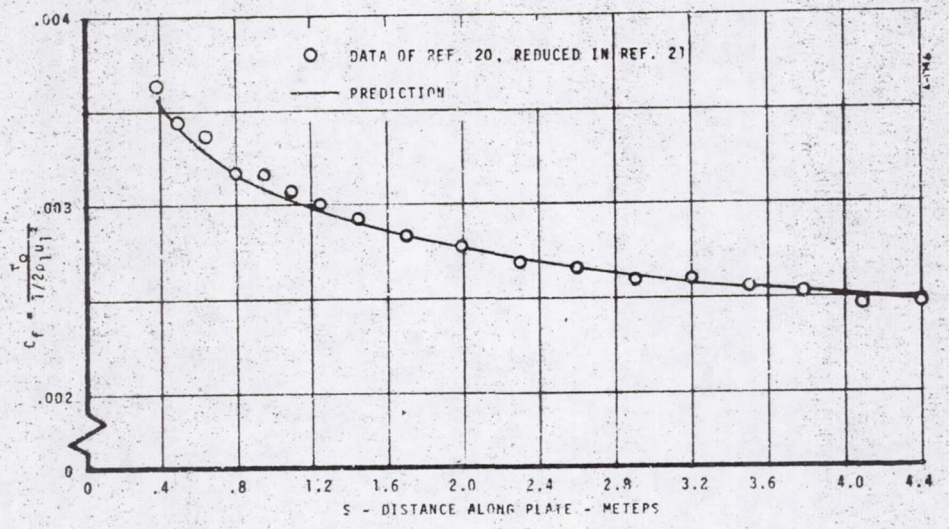

Figure 2a. Flat Plate Flow Comparison. 2-D Flow with No Blowing, No Pressure Gradient. Starting Profile Taken at S = 0.387 Meter

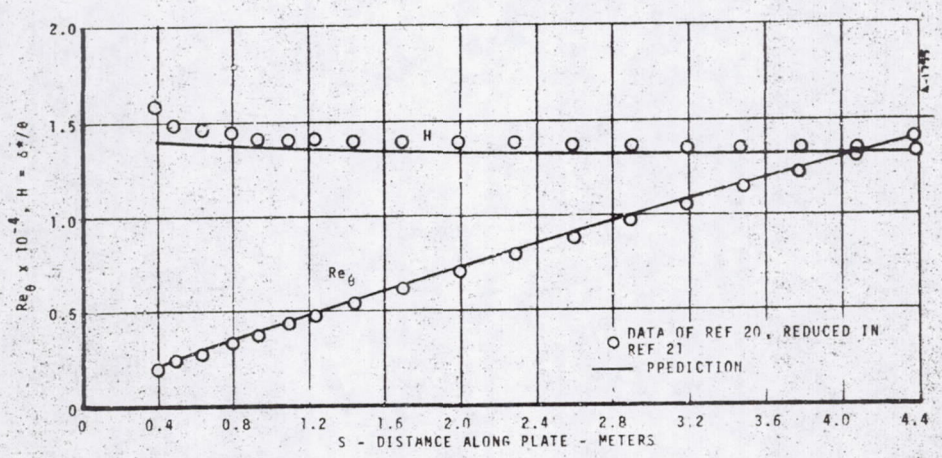

Figure 2b. Flat Plate Flow Comparison. 2-D Flow with No Blowing, No Pressure Gradient. Starting Profile Taken at S = 0.387 Meter

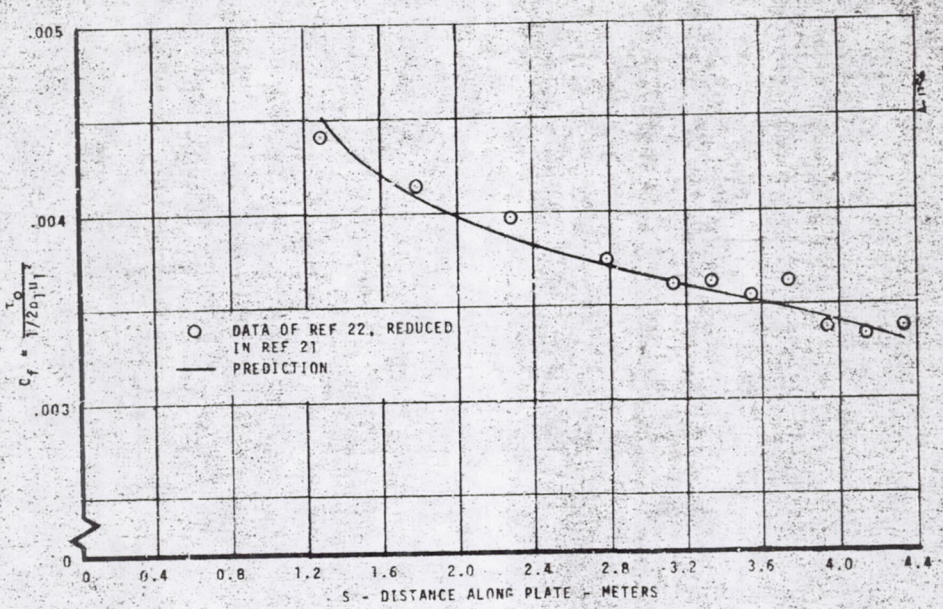

Figure 3a. Flow Comparison for Accelerating Flow. 2-D Flow with No Blowing. Starting Profile Taken at S = 1.282 Meters

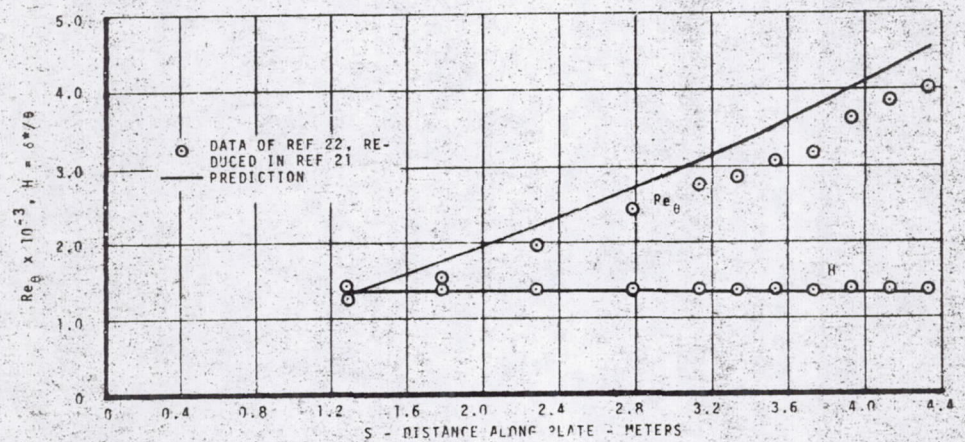

Figure 3b. Flow Comparison for Accelerating Flow. 2-D Flow with No Blowing. Starting Profile Taken at S = 1.282 Meters

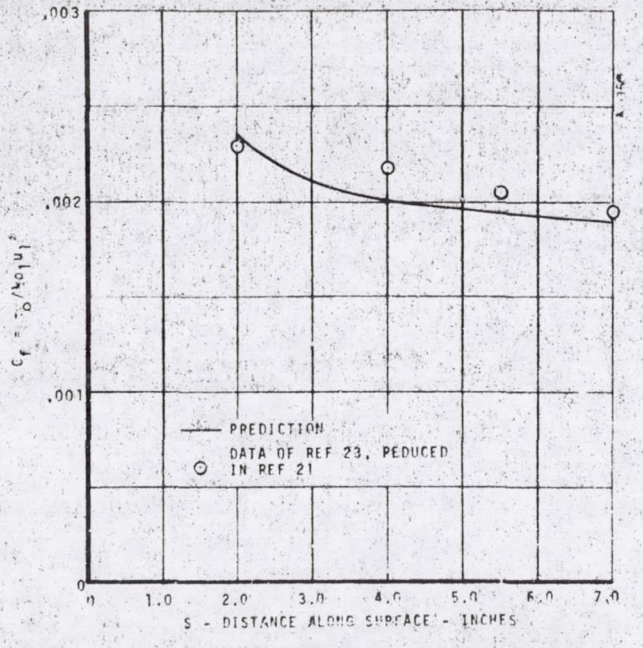

Figure 4a. Flow Comparison for Mild Positive Pressure Gradient. 2-D Flow with No Blowing. Starting Profile Taken at S = 2.0 Inches

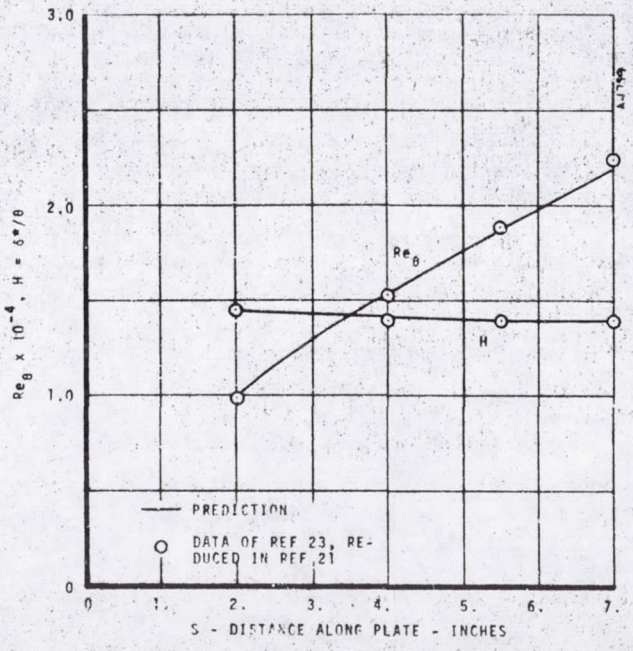

Figure 4b. Flow Comparison for Mild Positive Pressure Gradient. 2-D Flow with No Blowing. Starting Profile Taken at S = 2.0 Inches

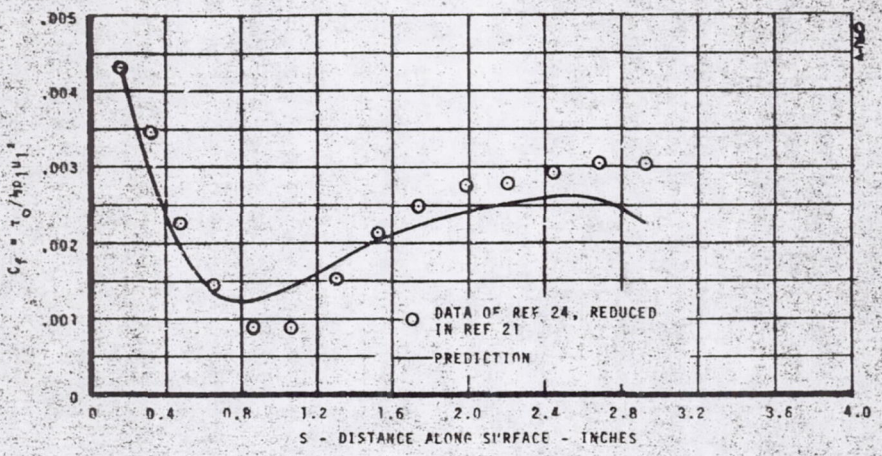

Figure 5a. Flow Comparison for Strong Pressure Rise Followed by Constant Pressure Relaxation. Axially Symmetric Flow with No Blowing. Starting Profile Taken at S = 0.162 Inch

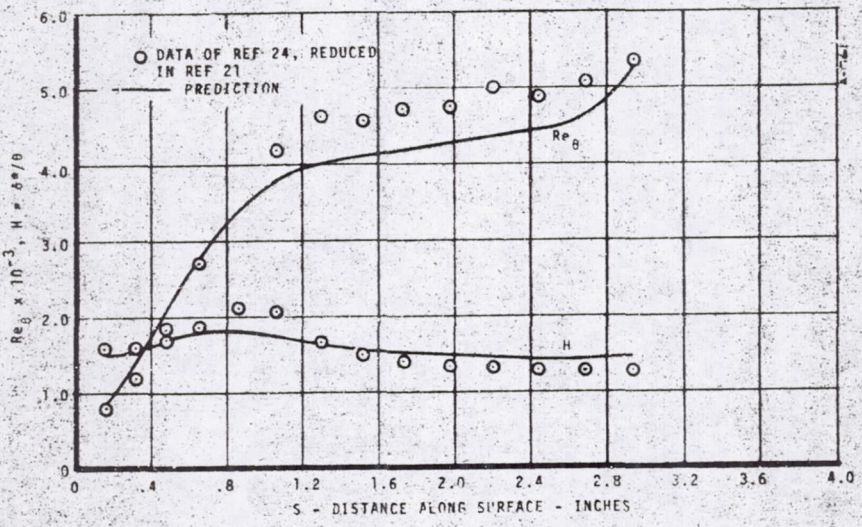

Figure 5b. Flow Comparison for Strong Pressure Rise Followed by Constant Pressure Relaxation. Axially Symmetric Flow with No Blowing. Starting Profile Taken at S = 0.162 Inch

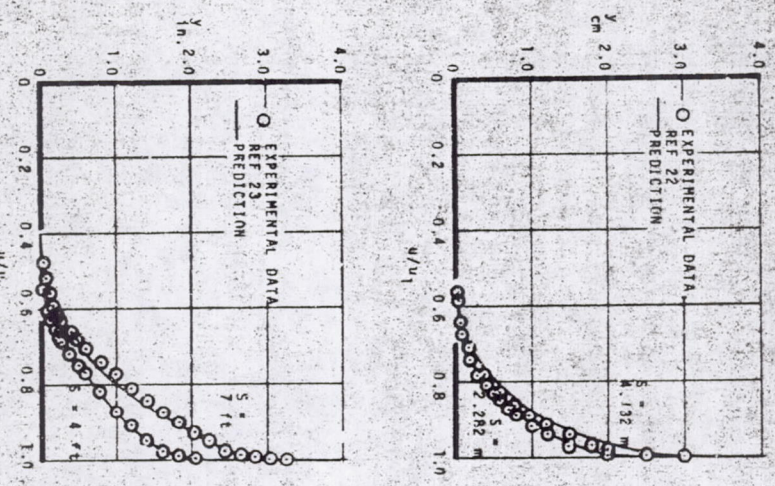

Figure 6. Typical Velocity Profiles

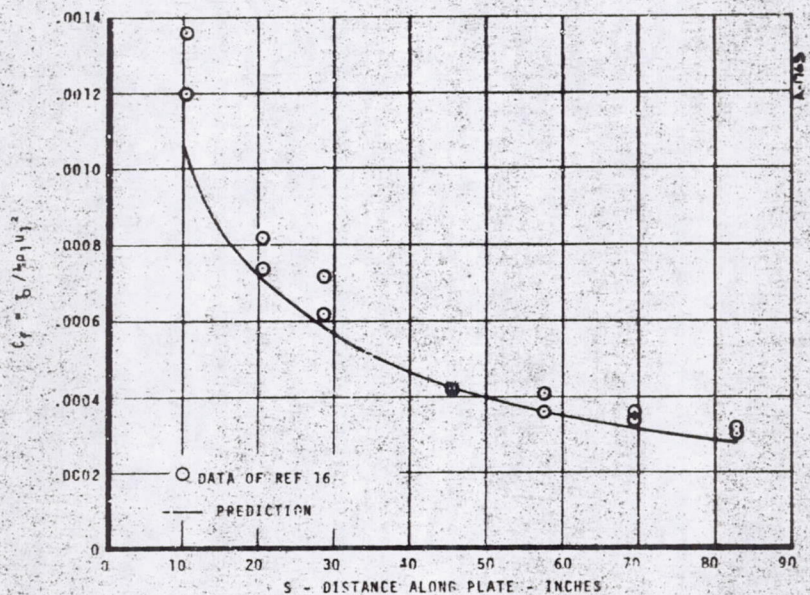

Figure 7. Flow Comparison for Flat Plate Flow, 2-D Flow, No Pressure Gradient, Strong Blowing (v_o/u_1 = 0.00543). Starting Profile Taken as Similar Solution at S = 1.00 Inch

slight shift of the curve to the right would perhaps reduce the error at several locations. This shift would be consistent with a profile matching based on θ rather than S, which has been postulated as being more correct (Reference 8). Nevertheless, drag coefficient predictions appear to be satisfactory. Finally, a velocity profile comparison is shown in Figure 8. Agreement with measured profile data is seen to be excellent.

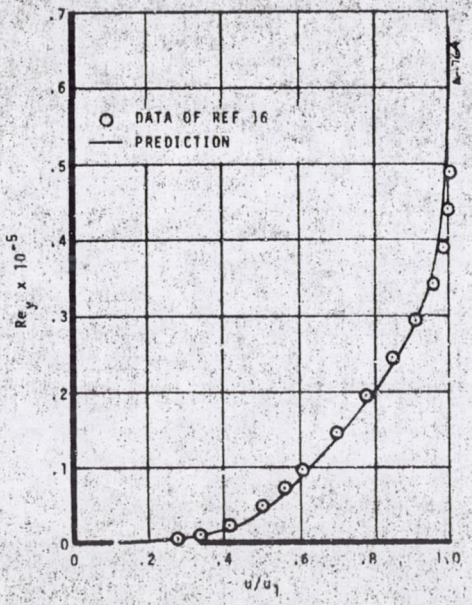

Figure 8. Velocity Profiles with Strong Blowing
$v_o/u_1 = 0.00543$
S = 45.3 Inches

REFERENCES

1. Kendall, R.M. and Bartlett, E.P.: Nonsimilar Solution of the Multicomponent Laminar Boundary Layer by an Integral-Matrix Method. AIAA Journal, Vol. 6, No. 6, June, 1968.

2. Pallone, A.J.: Nonsimilar Solutions of the Compressible-Laminar-Bourdary-Layer Equations with Applications to the Upstream-Transpiration Cooling Problem. J. Aerospace Sci., Vol. 28, No. 6, June 1961, pp. 449-456, 492.

3. Dorodnitsyn, A.A.: General Method of Integral Relations and Its Application to Boundary Layer Theory. Advances in Aeronautical Sciences, Vol. 3, Macmillan, New York, 1960, pp. 207-219.

4. Walsh, J.L., Ahlberg, J.H., and Nilson, E.N.: Best Approximation Properties of the Spline Fit. J. Math. and Mech., Vol. 11, 1962, pp. 225-234.

5. Leigh, D.C.F.: The Laminar Boundary Layer Equation: A Method of Solution by Means of an Automatic Computer. Cambridge Phil. Soc. Proc., Vol. 51, 1955, pp. 320-332.

6. Clauser, F.H.: The Turbulent Boundary Layer. Advances in Applied Mechanics, IV, pp. 1-51, 1956.

7. Klebanoff, P.S.: Characteristics of Turbulence in a Boundary Layer with Zero Pressure Gradient. NACA Technical Note 3178, 1954.

8. Kendall, R.M. Rubesin, M.W., Dahm, T.J., and Mendenhall, M.R.: Mass, Momentum, and Heat Transfer Within a Turbulent Boundary Layer with Foreign Gas Mass Transfer at the Surface, Part I - Constant Fluid Properties. Vidya Division, Itek Corporation, Final Report No. 111, 1964.

9. Reichardt, H.: Complete Representation of the Turbulent Velocity Distribution in Smooth Pipe. Z. Angew. Math. u. Mech., Vol. 31, No. 7, July 1951.

10. Rannie, W.D.: Heat Transfer in Turbulent Shear Flow. Jour. Aero. Sci., Vol. 23, No. 5, May 1956.

11. Deissler, R.G.: Analysis of Turbulent Heat Transfer, Mass Transfer, and Friction in Smooth Tubes at High Prandtl and Schmidt Numbers. NACA TN 3145, May 1954.

12. Rotta, J.: Velocity Law of Turbulent Flow Valid in the Neighborhood of a Wall. Ingr. Arch., Vol. 18, 1956, p. 277.

13. von Kármán, T.: The Analogy between Fluid Friction and Heat Transfer. Trans. ASME, Vol. 61, 1939, pp. 705-710.

14. van Driest, E.R.: On Turbulent Flow Near A Wall. Jour. Aero. Sci., Vol. 23, No. 11, November 1956.

15. Mickley, H.S., Curl, R., Gessner, A., and Ginwala, K.: Heat and Momentum Transfer for Flow Over a Flat Plate with Blowing and Main Stream Acceleration. M.I.T., NACA Contract Naw 6228.

16. Kendall, R.M.: Interaction of Mass and Momentum Transfer in the Turbulent Boundary Layer. Ph.D. Dissertation, M.I.T., 1959.

17. Bartlett, E.P., and Kendall, R.M.: Nonsimilar Solutions of the Multicomponent Laminar Boundary Layer by an Integral Matrix Method. Aerotherm Corporation Final Report No. 66-7, Part III, March 14, 1967.

18. Kendall, R.M., and Anderson, L.W.: Nonsimilar Solution of the Incompressible Turbulent Boundary Layer. Proceedings of the AFOSR-IFP-Stanford 1968 Conference on Turbulent Boundary Layer Prediction (to be published).

19. Abramowitz, M. and Stegun, I., editors: Handbook of Mathematical Functions with Formulas, Graphs, and Mathematical Tables. National Bureau of Standards, Applied Mathematics Series, 55. U.S. Govt. Printing Office, Washington, 1964.

20. Weighardt, K. and Tillman, W.: On the Turbulent Friction Layer for Rising Pressure. Translated in NACA TM 1314, 1951.

21. Kline, S.J., Cockrell,D.J., and Morkovin, M.V.: Proceedings of the AFOSR-IFP-STANFORD 1968 Conference on Turbulent Boundary Layer Prediction (to be published).

22. Ludwig, H., and Tillman, W.: Investigations of the Wall Shearing Stress in Turbulent Boundary Layers. Translated in NACA TM 1285, 1950.

23. Bradshaw, P.: The Turbulence Structure of Equilibrium Boundary Layers. NPL Aero. Report 1184, 1966.

24. Moses, H.L.: The Behavior of Turbulent Boundary Layers in Adverse Pressure Gradients. MIT Gas Turbine Laboratory Report No. 73, 1964.

APPENDIX A

THE SAINT BOUNDARY LAYER PROGRAM

A.1 GENERAL

The SAINT program (Strip Analysis for Incompressible Nonsimilar Turbulent boundary layers) generates velocity profiles and boundary layer parameters (drag coefficient, momentum and displacement thicknesses, shape factor, etc.), for the flow model described in the text of this report. Nonsimilar terms are retained in general; however, similar solutions within the context of the turbulent boundary layer transformation can also be obtained. At present, only incompressible, single component flows with or without injection can be solved. Turbulent intermittency can be considered; however, universally successful formulations of an intermittency function have not been found. Thus, intermittency has been neglected for all problems run to date.

The program requires a specification of the nodal network; streamwise stations at which a solution is desired; and edge velocity, velocity gradient and averaged* injection velocity at each of these stations. It also requires values for kinematic viscosity, intermittency factor, the Clauser parameter, $\varepsilon/u_1\delta^*$, and the two wall law constants y_a^+ and K. The program will accept an initial profile at the first station or will generate a similar profile.

The program can be used to solve laminar problems by setting the Clauser parameter, $\varepsilon/u_1\delta^*$, equal to zero. Care must be exercised in using this option, however, since the coordinate transformation is improper for laminar similar problems.

*The value read in at each station is the average of the injection velocity at that station and that at the previous station. This procedure allows proper description of discontinuous injection.

The program is presently dimensioned for up to 15 nodes in the boundary layer and 50 axial stations. Core requirements are approximately 30,000 octal words.

A.2 INPUT INSTRUCTIONS FOR THE SAINT BOUNDARY LAYER PROGRAM

Card Set 1 - Control card (KR values) and title. Format 20I1, 15A4

Column 1 - Determines whether a new set of eta values is to be input for the present case.

0	use resident values from previous case
1	values input by user (mandatory for first case)

Column 2 - Designates method for obtaining first guesses for primary variables

0	use resident values from previous case
1	use built-in relations to calculate first guesses
2,3	read in profile supplied by user
3	accept profile as station 1 solution and proceed to IS = 2

Column 3 - Determines treatment of streamwise derivatives

0	perform similar solution at each streamwise station
1	consider two-point difference relations at all stations with the following exceptions (a similar solution is performed at the first station for nonblunt bodies and at the first two stations for blunt bodies).
2	consider three-point difference relations at all stations with the following exceptions (a similar solution is performed at the first station and a two-point solution is performed at the second station for nonblunt bodies, similar solutions are performed at the first and second stations and a two-point solution is performed for the first station after a discontinuity.

Column 4 - Determines when output block is to be printed

0	output block printed for converged solution or for non-converged solution after 50 iterations (with appropriate comment)
1	output block printed after each iteration

Column 5 - Not used

Column 6 - Not used

Columns 7-20 - Not used at present

Columns 21-80 - Case name (alphanumeric). Used for identification of printed output

Card Set 2 - Axial stations at which data will be read in and output block will be printed

Card 1 - NS, format I2. Number of stations. Up to 50 stations can be considered.

Card 2 - S, format 8E10.4. Stations. A negative entry for S signifies a discontinuity at that station. This produces a two-point difference solution at the first station after the discontinuity and thus has an effect only for three-point solutions (KR(3)=2).

Card Set 3 - Eta and intermittency values

Card 1 - NETA, format I2. Number of eta values.

Card(s) 2-ETA, format 8E10.4. Eta values. Up to 15 points can be considered across the boundary layer.

Card(s) 3-PHI, format 8E10.4. Turbulent intermittency value at each eta. If intermittency is not to be considered, enter 1.0 NETA times.

Card Set 4 - Program constants cards

Card 1 - Format I2, 2E10.4, I3

Column 1-2 - KAPPA. The node at which u/u_1 is fixed at a given value.

Column 3-12- CBAR. The value of u/u_1 at the KAPPA node.

Column 13-22-$\frac{\varepsilon}{u_1 \delta^*}$. The value to be used for the Clauser parameter. If left blank or entered as a zero, a laminar solution will be obtained.

Column 23-25-NBEND. The value of n in the expression $\varepsilon = \frac{\varepsilon_1 \varepsilon_2}{\left(\varepsilon_1^n + \varepsilon_2^n\right)^{1/n}}$. A value of 5 is typically used.

Card 2 - Format 8E10.4

Column 1-10- K. This is the constant K in the mixing length equation.

Column 11-20-YA2. This constant (y_a^+) also appears in the mixing length equations.

Card Set 5 - Freestream, viscosity, and mass injection information

Card(s) 1 - UE, format 8E10.4. Freestream velocity at each station.

Card(s) 2 - DUDS, format 8E10.4. Freestream velocity gradient at each station.

Card(s) 3 - VISC, format 8E10.4. Kinematic viscosity at each station.

Card(s) 4 - VW, format 8E10.4. Mass injection rate at each station averaged with the value at the previous station.

Card Set 6 - Initial Conditions. Format 8E10.4 (include if KR(2) = 2 or 3).

Column 1-10 - ALPH. Initial alpha

Column 11-20- f_1. Value of stream function at wall (usually zero). Program will compute its own value for problems with blowing or suction.

Column 21-30- (f_1''/α^2)

Column 31-40- (f''_{edge}/α^2). Enter a zero here.

Columns 41-80 and following cards - u/u_1 for each eta.

A.3 INPUT FOR A SAMPLE CASE

```
1321                    MOSES CASE 5 - 4000
a
.162      .323      .484      .646      .865      1.059     1.303     1.516
13
0.        .0139     .0346     .0691     .1152     .264      .387      .540
.694      .846      1.00      1.153     2.0
1.        1.        1.        1.         1.       1.        1.        1.
1.        1.        1.        1.        1.
11 .9870     .019        5
.44       11.83
76.26     69.09     61.38     55.49     51.14     49.54     48.93     48.65
-40.2     -42.      -47.      -27.5     -14.      -6.2      0.        0.
.000166   .000166   .000166   .000166   .000166   .000166   .000166   .000166
0.        0.        0.        0.        0.        0.        0.        0.
.0841     0.        159.      0.        0.        .181      .375      .524
.635      .728      .779      .844      .905      .955      .987      .996
1.00
```